conductivity is not an important conductivity mechanism in the lower mantle. He calculated the temperature T_c where ionic conductivity equals electronic conductivity for an olivine-dominated mantle, as a function of pressure. He found that T_c is significantly higher than projected mantle temperatures [D. C. Tozer, *Phys. Chem. Earth* **3**, 414 (1959)].

23. X. Li and R. Jeanloz, *Geophys. Res. Lett.* **14**, 1075 (1987); J. Peyronneau and J. P. Poirier, *Nature* **342**, 537 (1989); X. Li and R. Jeanloz, *J. Geophys. Res.* **95**, 5067 (1990); *Nature* **350**, 332 (1991); B. J. Wood and J. Nell, *ibid.* **351**, 309 (1991); X. Li et al., *J. Geophys. Res.* **98**, 501 (1993).
24. N. F. Mott and R. W. Gurney, *Electronic Processes in Ionic Crystals*, (Dover, New York, 1964).
25. J. Ducruix, V. Courtillot, J. L. Mouel, *Geophys. J. R. Astron. Soc.* **61**, 73 (1980).
26. References for data in Table 1 are as follows: for nepheline and diopside, C. Connolly and K. Muehlenbachs, *Geochim. Cosmochim. Acta* **52**, 1585 (1988); melilite, T. Hayashi and K. Muehlenbachs, *ibid.* **50**, 585 (1986); anorthite, S. C. El-
phick, C. M. Graham, P. E. Dennis, *Contrib. Mineral. Petrol.* **100**, 490 (1988); forsterite, K. Ando, H. Kurokawa, Y. Oishi, *J. Am. Ceram. Soc.* **64**, C30 (1981) and O. Jaoul, B. Houlier, F. Abel, *J. Geophys. Res.* **88**, 613 (1983); quartz, P. F. Dennis, in *Progress in Experimental Petrology*, C. M. B. Henderson, Ed. (Cambridge Univ. Press, Cambridge, 1984), p. 260; SiO_2 glass, H. A. Schaeffer and K. Muehlenbachs, *J. Mater. Sci.* **13**, 1146 (1978); Mg-spinel, K. Ando, Y. Oishi, *J. Chem. Phys.* **61**, 625 (1974); Mg-spinel, K. P. R. Reddy and A. R. Cooper, *J. Am. Ceram. Soc.* **64**, 368 (1981); MgO and α-Fe_2O_3, K. P. R. Reddy and A. R. Cooper, *ibid.* **66**, 664 (1983); and sapphire, K. P. R. Reddy and A. R. Cooper, *ibid.* **65**, 634 (1982).
27. We thank T. Chacko, R. W. Luth, J. Farquhar, J. Staveley, and two anonymous reviewers for constructive comments and O. Levner for assistance with analyses. Supported by the Natural Sciences and Engineering Research Council of Canada.

The Relation Between Biological Activity of the Rain Forest and Mineral Composition of Soils

Y. Lucas,* F. J. Luizão, A. Chauvel, J. Rouiller, D. Nahon

In most soils of the humid tropics, kaolinitic topsoil horizons overlie more gibbsitic horizons. This arrangement cannot be produced simply by leaching. Quantitative measurement of the turnover of chemical elements in the litterfall in an Amazonian ecosystem indicates that the forest cycles a significant amount of elements, particularly silicon. As a result, fluids that percolate through topsoil horizons already contain dissolved silicon. This effect keeps silicon from being leached down and may account for the stability of kaolinite in the soil upper horizons. The soil mineral composition is thus maintained by biological activity.

Tropical acid soils are composed of residual primary minerals, mainly quartz grains (SiO_2), and newly generated secondary minerals, mainly kaolinite [$Al_2Si_2O_5(OH)_4$] and smaller quantities of gibbsite [$Al(OH)_3$], hematite (Fe_2O_3), and geothite ($FeOOH$). In most of the well-drained, nonspodic acid soils under tropical humid climates, kaolinite is the prevailing secondary mineral in the topsoil horizons. The observed gibbsitic horizons appear to be situated beneath more kaolinitic horizons as gibbsitic saprolite, nodular or bauxitic horizons, or gibbsite accumulations in a kaolinitic matrix (*1–3*). From a chemical standpoint, these soils are more siliceous on the top horizons and more aluminous underneath. This structure of the soil profile is observed for old soils, such as Amazonian bauxites, as well as for young soils.

Y. Lucas, Núcleo de Pesquisa da Geoquímica da Litosfera and Institut Français de Recherche Scientifique pour le Développement en Coopération, Université de São Paulo, CP 9638, 01065 São Paulo, Brazil.
F. J. Luizão and A. Chauvel, Instituto Nacional de Pesquisas da Amazônia, Laboratório de Ecologia, CP 478, 69060 Manaus, Brazil.
J. Rouiller, Centre de Pédologie Biologique, 54500 Vandoeuvre-les-Nancy, France.
D. Nahon, Université Saint-Jérôme, Géosciences de l'Environnement, 13397 Marseille Cedex 13, France.

*To whom correspondence should be addressed.

This observed vertical succession is just the opposite of that predicted by most geochemical soil formation models (*4–7*). These models take a low-Si and -Al rainwater input on topsoil into consideration. As the water percolates, the solution-mineral reactions lead to a progressive increase of the Si and Al concentration in the soil solution. The models predict a vertical succession of horizons, with more aluminous gibbsitic horizons in the topsoil above the more siliceous kaolinitic horizons. The discrepancy between the models and the observed soil horizons has long been ignored for two reasons. There has been a lack of field studies on humid tropical soil geochemistry, and the top horizons of tropical soils have been frequently interpreted as allochtonous, that is, the kaolinitic material was deposited after the lower soil layers had formed. Numerous studies in the last 20 years, however, have pointed out that such allochtony is more restricted than had been thought. Most of the tropical soils have formed in situ (*8, 9*), with a possible input of foreign material by dust deposition (*10*). Various other explanations of the siliceous topsoil production have already been proposed: uplift of deep material by termites or ants (*11*); rapid percolation of the rainwater

through the topsoil so that water-mineral interaction does not reach equilibrium (*12*); or decreased water activity in the topsoil during dry seasons, displacing the kaolinite-gibbsite equilibrium (*13*). These hypotheses rarely apply to humid tropical soils, however. Termite or ant activity is normally restricted to the upper horizons of soil where the dry season is short. Water generally percolates slowly through soils as capillary water (*14*). During exceptionally dry periods, soil suction can reach 15 bars, which is the usually accepted limit for plant wilting. Under these conditions, maximum water activity changes would be from 1 to 0.989, which correspond to a quite small (+0.55%) shift of the dissolved SiO_2 concentration at the gibbsite-kaolinite equilibrium.

To investigate the source of this permanent Si stock above more aluminous horizons, we studied the role of the rain forest itself on the geochemical cycling of the elements that act on the mineral-solution reactions, paying special attention to Si. The potential effect of plants on element cycles in soils has long been apparent (*15, 16*), but only limited data are available for Si or Al (*17, 18*), especially in the tropics. Here we evaluate the element turnover in the forest annual litterfall and the total Si content of the forest, as well as the potential influence of elemental cycling in the forest on soil mineral composition.

Our study site was 80 km north of Manaus, Brazil ($02°34'S$, $60°07'W$). The climate is equatorial; average annual rainfall is 2100 mm and the dry season lasts 3 months. The landscape is a plateau covered by a typical Amazonian rain forest (*19*). Soils (*20*) consist of a 3- to 8-m-thick kaolinitic clay overlying a more gibbsitic 3-m-thick nodular horizon (Fig. 1). The mean ratio of kaolinite to gibbsite decreases from 14 in the upper clay to 3 in the nodular horizon. These soils were formed by a progressive desilicification of the sandy-clay parent sediment. The progressive ver-
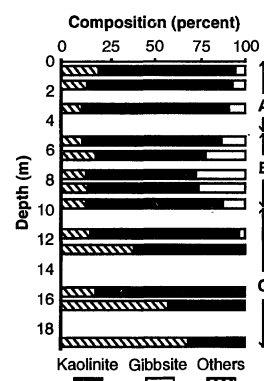

Fig. 1. Mineralogical composition of the soils. (**A**) Upper clay horizon, (**B**) nodular horizon, and (**C**) saprolite.

tical variation of shape, size, crystallography, and crystal chemistry of the kaolinites attests to the in situ geochemical differentiation of the whole profile (3, 21), and gibbsite is currently formed underneath the thick kaolinitic upper horizon (22).

We sampled litterfall in conical traps for 2 years (23), on a weekly basis during the rainy season and sometimes on a bimonthly

Fig. 2. Silicon cycling in the equatorial rain forest. Numbers in parentheses are in kilograms per hectare per year.

basis during the dry season. Samples were sorted into leaves, reproductive parts (flowers, fruits, and seeds), fine woody material, and residue. Animal material and scarce-adhering mineral material were discarded. After sorting, samples were dried, weighed, finely ground, and stored. A bulk sample for the entire 2-year litterfall was used for chemical analysis (24). No correction was made for possible mass or element losses during the time the litter was in the trap.

The mean litterfall weight for the 2 years of collection was 8.4 tons ha^{-1} $year^{-1}$. The elements Ca and Si dominated the litterfall element concentrations, 4.4 and 4.0 per mil, respectively, followed by K, Mg, Al, Na, Fe, P, Mn, and Ti, in decreasing order of relative concentration (Table 1). The element Si was mainly concentrated in the leaves, whereas Ca was more evenly distributed among the different components. The elements Al, Fe, and Ti were mainly concentrated in the residue, which may represent soil material brought up to the trees by termites. The annual Ca and Si turnover in the litterfall was 36 and 33 kg ha^{-1} $year^{-1}$, respectively, and the annual turnover of other elements was less (Table 2). The possible recycling by termites of soil material through the residue fraction is <0.8 kg ha^{-1} $year^{-1}$ for Si. The SiO_2/Al_2O_3 ratio of the annual litterfall was >10, whereas in the first meter of soil it was less than 1.3 (bulk soil) or 1.1 (kaolinite plus gibbsite).

We estimated the total Si content of the forest by using existing data on floristic

composition, average phytomass of the aerial parts (trunks, branches, and leaves) (25), and Si content in trunks and litterfall fractions. The 235 tree species listed in the forest represent a trunk volume of 287 m^3 ha^{-1} (19). Wood density and Si content data were available for 39 species (26), which represent a trunk volume of 120 m^3 ha^{-1}; the average trunk density is 0.75 ton m^{-3}, and the average Si content is 3.34 per mil. The trunk Si content of these 39 species is 301 kg ha^{-1}, which may be considered a minimum value for Si content of the forest. If we extrapolate to the whole forest, using the average Si content calculated from the 39 species and the average leaf and branch Si content measured in the litterfall, the value is 834 kg ha^{-1} (Table 3). This Si content could be considered a reasonable estimate for the above-ground parts of the forest.

This value is low compared with the Si stock in soil kaolinites, which is >3000 tons ha^{-1} for the top 3 m of soil in our study site. The absolute value of the forest Si stock tells us nothing about the Si turnover by root uptake and input from litterfall, stemflow, and throughfall. The Si turnover in the fine litterfall that we measured was 33 kg ha^{-1} $year^{-1}$. The turnover due to the coarse woody litterfall (trees and branches) is 8 kg ha^{-1} $year^{-1}$, if the annual renewal rate of the aerial parts is 1% (27). Negating the Si from stemflow and throughfall, which are important sources of topsoil input for nutrients (28), we obtain 41 kg ha^{-1} $year^{-1}$ as the minimum total Si turnover by the rain forest.

This value has to be compared to the amount of Si that is annually leached out of the soils. This content can be calculated from the mean Si concentration in stream waters that drain the studied area, 2.1 mg $liter^{-1}$ (29), and from the amount of water that annually percolates through the soils, 500 mm. The latter value is equal to the annual rainfall minus the evapotranspiration. The surface runoff and the litter washed out of the system by the streams are negligible in plateau areas (30). From these data, the amount of Si leached out of the weathering zone is ~11 kg ha^{-1} $year^{-1}$.

Thus, the Si input (41 kg ha^{-1} $year^{-1}$) from the rain forest on top of the soil is about four times greater than the Si leached
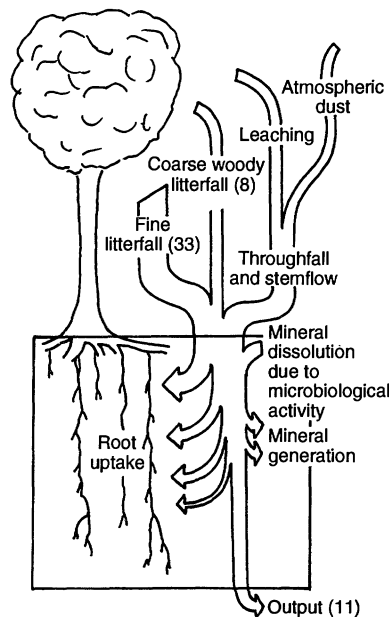
Table 1. Composition of the average annual litterfall. Values in per mil for all elements, in kilograms per hectare for the dry weight. Composition of total fine litterfall was calculated from composition of each fraction related to its dry weight.

Source	Component										
	Si	Al	Fe	Mn	Mg	Ca	Na	K	Ti	P	Dry weight
Leaves	5.5	0.35	0.03	0.10	1.6	3.9	0.73	1.6	0.01	0.11	5.64
Reproductive parts	0.40	0.10	0.21	0.05	1.3	2.5	0.20	5.3	0.01	0.34	0.40
Wood	0.98	0.37	0.06	0.09	1.1	6.0	0.26	1.4	0.05	0.08	1.55
Residue	1.0	1.6	1.0	0.10	1.5	5.5	0.23	2.2	0.13	0.36	0.81
Total fine litterfall	4.0	0.46	0.14	0.09	1.5	4.4	0.57	1.8	0.03	0.14	8.40

Table 2. Annual turnover due to the litterfall. Values in kilograms per hectare per year.

Source	Component									
	Si	Al	Fe	Mn	Mg	Ca	Na	K	Ti	P
Leaves	30.8	2.0	0.19	0.55	9.2	22.0	4.1	8.9	0.04	0.61
Reproductive parts	0.16	0.04	0.08	0.02	0.52	0.99	0.08	2.1	0.00	0.14
Wood	1.5	0.57	0.10	0.14	1.8	9.3	0.40	2.2	0.07	0.13
Residue	0.81	1.3	0.83	0.08	1.2	4.4	0.19	1.8	0.11	0.29
Total fine litterfall	33.3	3.9	1.2	0.79	12.7	36.7	4.8	15.0	0.22	1.2

Table 3. Silicon content of the Amazonian forest. Total Si content was 834 kg ha^{-1}

	Weight of fraction (ton ha^{-1})	Si content (per mil)	Si content (kg ha^{-1})
Trunks	214	3.3	715
Branches	95	1.0	93
Leaves	4.8	5.5	26

out of the system (11 kg ha^{-1} year^{-1}). If we neglect input from forest renewal, stemflow, throughfall, and aerial dust, the annual average concentration of Si and Al in the solution that leaches the litterfall is 5.65 and 0.65 μmol liter^{-1}, respectively. In consideration of solubility diagrams (31), we find that such a water is supersaturated with Si with respect to kaolinite for a pH of 5.1 or greater.

Thus, geochemical modeling of soil formation and weathering in equatorial areas must be considered (Fig. 2). Topsoil inputs of elements, especially Si and Al, are significant. They are added mainly in fine litterfall, larger litterfall (tree and branch felling), throughfall, and stemflow. The last two fractions may include an appreciable amount of atmospheric dust transported from great distances (32). In the top meter of the soil, microbiological activity leads to a dissolution of soil minerals, which increases Si and Al concentrations (33). As the solution percolates through the soil, the Al and Si concentrations are mainly controlled by root uptake and mineral-solution interactions. Kaolinite is stable in the upper part of the soil, and gibbsite precipitates in depth. These interactions should be included in models of soil water and stream-water chemistry.

REFERENCES AND NOTES

1. J. Delvigne, *Mémoire 13* (Office de la Recherche Scientifique et Technique Outre-Mer, Paris, 1965).
2. G. Sieffermann, *Mémoire 66* (Office de la Recherche Scientifique et Technique Outre-Mer, Paris, 1969).
3. Y. Lucas, A. Chauvel, J. P. Ambrosi, in *Geochemistry and Mineral Formation in the Earth Surface,* R. Rodriguez-Clemente and Y. Tardy, Eds. (Consejo Superior de Investigaciones Cientificas, Madrid, 1986) pp. 289–299.
4. B. Fritz and Y. Tardy, *Sci. Geol. Bull.* **26**, 339 (1973).
5. C. Fouillac and G. Michard, *Geochim. Cosmochim. Acta* **41**, 207 (1977).
6. A. C. Lasaga, *J. Geophys. Res.* **89**, 4009 (1984).
7. J. P. Ambrosi, thesis, Poitiers University (1990).
8. P. Lecomte, *J. Geochem. Explor.* **30**, 35 (1988).
9. C. R. M. Butt, in *Handbook of Exploration Geochemistry,* G. J. S. Govett, Ed. (Elsevier Amsterdam, 1992), vol. 4, chap. I.6.
10. G. H. Brimhall *et al., Science* **255**, 695 (1992).
11. P. Nye, *J. Soil Sci.* **6**, 73 (1955).
12. B. I. Kronberg *et al., Chem. Geol.* **35**, 311 (1982).
13. Y. Tardy and A. Novikoff, *C. R. Acad. Sci. Paris* **306-II**, 39 (1988).
14. K. Rozanski *et al., SM-313* (International Atomic Energy Agency, Vienna, 1991).
15. T. S. Lovering, *Geol. Soc Am. Bull.* **70**, 781 (1959).
16. A. J. Herbillon, in *Soils with Variable Charge,* B. K. G. Theng, Ed. (New Zealand Society of Soil Science, Lower Hutt, 1980), pp. 109–126.
17. F. Bartoli, *Sci. Geol. Bull.* **39**, 195 (1986).
18. M. Gautam-Basak and J. Proctor, *Malays. For.* **46**, 224 (1983).
19. G. T. Prance, W. A. Rodrigues, M. F. Da Silva, *Acta Amazonica* **6**, 9 (1976). This work provides an exhaustive quantitative study (floristic composition and trunk volume) of the Manaus plateau forest.
20. According to different classifications, soils are Xanthic Ferralsols [*Soil Map of the World,* (Food and Agriculture Organization, Rome, 1975)], Aplic Ac-

rortox (*Soil Taxonomy,* Agricultural Handbook 436 (U.S. Department of Agriculture, Washington, DC, 1975)], or Yellow latossols [(*Sistema de Classificao dos Solos,* (Empresa Brasileira de Pesquisa Agropecuária, Rio de Janeiro, 1979)].
21. G. Irion, *Monogr. Biol.* **56**, 537 (1984).
22. Y. Lucas, B. Kobilsek, A. Chauvel, *Trav. Com. Int. Etude Bauxites Alum. Alum.* **19**, 81 (1989).
23. Fifteen 80-cm conical litter traps were placed at random on the 140-m diagonal of a 1-ha plot. Samples were taken from August 1980 to September 1982.
24. Analyses were obtained at the Centre de Pédologie Biologique, Nancy, France. Samples were calcinated at 500°C and dissolved by strontium metaborate melting. They were then analyzed by plasma emission spectrometry for Si, Al, Fe, Mn, Mg, Ca, Ti, and P and by atomic absorption spectrometry for K and Na. Results were corrected from the loss of weight at 1000°C.
25. The phytomass of trunks, branches, and leaves was estimated by the method proposed by J. P. Lescure *et al.* [*Acta Oecol. Oecol. Gen.* **4**, 237 (1983)].
26. The species with both Si content and density available were *Aspidosperma album,** *Scleronema micranthum,*† *Protium insigne,** *Protium* sp.,* *Tretragastris* sp.,* *Swartzia reticulata,** *Eperua bijuga,** *Macrolobium* sp.,* *Swartzia panacoco,*† *Caryocar palidum,** *Cecropia* sp.,* *Pourouma cecropiifolia,** *Couepia canomensis,** *Lycania heteromorpha,** *Lycania* ind.,* *Parinari excelsa,** *Buchenavia* sp.,* *Andira unifoliata,** *Dipteryx odorata,*† *Laetia procera,** *Licaria aritu,*†

Licaria aurea,* *Nectandra rubra,** *Eschweilera odora,*† *Eschweilera* sp.,* *Mouriria* sp.,* *Guarea* sp.,* *Inga* sp.,* *Brosimum* sp.,* *Ficus* sp.,* *Helicostylis* sp.,* *Virola calophylla,*† *Minquartia guianensis,** *Ecclinusa bacuri,** *Pouteria* sp.,* *Prieurella* sp.,* *Erisma* sp.,* *Qualea paraensis,*† and *Qualea* sp.* Data from species marked with an asterisk are from *Taux de Silice dans Différents Bois Amazoniens* (Laboratoire de Chime du Bois du Centre Technique Forestier Tropical, Nogent-sur-Marne, France, 1990), and those marked by a dagger are from *Estudo de 55 Espécies Lenhosas para Geração de Energia em Caldeiras* (Lab. Quimica da Madeira, Instituto Nacional de Pesquisa da Amazônia, Manaus, Brazil, 1986).
27. F. Hallé, R. A. A. Oldeman, P. B. Tomlison, *Tropical Trees and Forests: An Architectural Analysis* (Springer-Verlag, New York, 1978).
28. M. C. Forti and L. M. Moreira-Nordemann, *J. Geophys. Res.* **96**, 7415 (1991).
29. K. Furch, *Monogr. Biol.* **56**, 167 (1984).
30. W. Franken and P. R. Leopoldo, *ibid.,* p. 501.
31. L. R. Gardner, *Am. Mineral.* **55**, 1380 (1970).
32. R. Swap *et al., AMS 19th Conference on Hurricane and Tropical Meteorology,* Miami, May 1991 (American Meteorological Society, Boston, 1991), pp. 30–34.
33. A. Chauvel, F. Andreux, C. C. Cerri, *Trav. Com. Int. Etude Bauxites Alum. Alum.* **19**, 45 (1989).
34. We thank J. Proctor, B. Forsberg, C. Forti, and A. Herbillon for improving the text and for their constructive remarks.

8 September 1992; accepted 24 December 1992

Record Low Global Ozone in 1992

J. F. Gleason, P. K. Bhartia, J. R. Herman, R. McPeters, P. Newman, R. S. Stolarski, L. Flynn, G. Labow, D. Larko, C. Seftor, C. Wellemeyer, W. D. Komhyr, A. J. Miller, W. Planet

The 1992 global average total ozone, measured by the Total Ozone Mapping Spectrometer (TOMS) on the Nimbus-7 satellite, was 2 to 3 percent lower than any earlier year observed by TOMS (1979 to 1991). Ozone amounts were low in a wide range of latitudes in both the Northern and Southern hemispheres, and the largest decreases were in the regions from 10°S to 20°S and 10°N to 60°N. Global ozone in 1992 is at least 1.5 percent lower than would be predicted by a statistical model that includes a linear trend and accounts for solar cycle variation and the quasi-biennial oscillation. These results are confirmed by comparisons with data from other ozone monitoring instruments: the SBUV/2 instrument on the NOAA-11 satellite, the TOMS instrument on the Russian Meteor-3 satellite, the World Standard Dobson Instrument 83, and a collection of 22 ground-based Dobson instruments.

The Nimbus-7 TOMS (Total Ozone Mapping Spectrometer) has observed the amount and distribution of atmospheric total column ozone since November 1978. From 1979 to 1991, the amount of total column ozone has decreased over most of globe (1–3). Small (3 to 5%) losses at mid-latitudes, larger (6 to 8%) losses at high latitudes, and no losses near the equator were reported (2, 3). The most dramatic ozone decease has been observed each year in the springtime Antarctic ozone hole region (4) and the 1992 ozone amounts there were about 50% of the 1979 amounts.

For latitudes between 65°S and 65°N, the average area-weighted ozone loss rate

for all seasons (1979 to 1991), after correction for solar cycle and quasi-biennial oscillation (QBO) effects has been estimated to be 2.7 ± 1.4% per decade (1–3). Analysis of the 13-year ozone data shows that most of the ozone depletion has occurred at mid- and high latitudes (2, 3). In this report we examine the decrease in the global daily average ozone amount from 1992 into 1993. We show that the observed decrease is consistent with measurements from other satellite and ground-based instruments.

The TOMS data show that the 1992 daily global average (65°S to 65°N) total ozone amount is significantly lower than in any of the earlier 13 years. The daily global